GL-TR-89-0207   **AD-A214 987**

Enhanced Satellite Geodesy Through the
Addition of a Pseudorange Observable

Jayant Sharma

Massachusetts Institute of Technology
77 Massachusetts Avenue
Cambridge, MA 02139
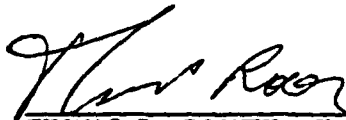
May 1989

Scientific Report No. 4

APPROVED FOR PUBLIC RELEASE; DISTRIBUTION UNLIMITED

DTIC
S ELECTE
DEC 0 7 1989
E D

This technical report has been reviewed and is approved for publication.

THOMAS P. ROONEY, Chief
Contract Manager
Geodesy and Gravity Branch

FOR THE COMMANDER

DONALD H. ECKHARDT, Director
Earth Sciences Division

This report has been reviewed by the ESD Public Affairs Office (PA) and is releasable to the National Technical Information Service (NTIS).

Qualified requestors may obtain additional copies from the Defense Technical Information Center. All others should apply to the National Technical Information Service.

If your address as changed, or if you wish to be removed from the mailing list, or if the addressee is no longer employed by your organization, please notify GL/IMA, Hanscom AFB, MA 01731-5000. This will assist us in maintaining a current mailing list.

Do not return copies of this report unless contractual obligations or notices on a specific document requires that it be returned.

SECURITY CLASSIFICATION OF THIS PAGE

REPORT DOCUMENTATION PAGE

1a REPORT SECURITY CLASSIFICATION UNCLASSIFIED	1b RESTRICTIVE MARKINGS N/A
2a SECURITY CLASSIFICATION AUTHORITY	3 DISTRIBUTION / AVAILABILITY OF REPORT
2b DECLASSIFICATION / DOWNGRADING SCHEDULE	Approved for public release; distribution unlimited.
4 PERFORMING ORGANIZATION REPORT NUMBER(S)	5 MONITORING ORGANIZATION REPORT NUMBER(S) GL-TR-89-0207

6a NAME OF PERFORMING ORGANIZATION Massachusetts Institute of Technology	6b OFFICE SYMBOL (If applicable) Room 37-552	7a NAME OF MONITORING ORGANIZATION Geophysics Laboratory
6c ADDRESS (City, State, and ZIP Code) 77 Massachusetts Avenue Cambridge, MA 02139		7b ADDRESS (City, State, and ZIP Code) Hanscom Air Force Base, MA 01731-5000

8a. NAME OF FUNDING / SPONSORING ORGANIZATION Air Force Geophysics Laboratory	8b OFFICE SYMBOL (If applicable) AFGL/LWG	9 PROCUREMENT INSTRUMENT IDENTIFICATION NUMBER F19628-86-K-0009

8c ADDRESS (City, State, and ZIP Code)

Hanscom Air Force Base, MA 01731-5000

10. SOURCE OF FUNDING NUMBERS

PROGRAM ELEMENT NO	PROJECT NO	TASK NO	WORK UNIT ACCESSION NO
61102F	2309	G1	BN

11 TITLE (Include Security Classification)

Enhanced Satellite Geodesy Through The Addition of a Pseudorange Observable

12 PERSONAL AUTHOR(S) Jayant Sharma

13a TYPE OF REPORT Scientific #4	13b TIME COVERED FROM 86 Apr TO 89 May	14 DATE OF REPORT (Year, Month, Day) 1989 May	15 PAGE COUNT 50

16 SUPPLEMENTARY NOTATION
Submitted to M.I.T. Dept. of Aeronautics and Astronautics in partial fulfillment of the requirements for the degree of Master of Science

17 COSATI CODES			18 SUBJECT TERMS (Continue on reverse if necessary and identify by block number)
FIELD	GROUP	SUB-GROUP	NAVSTAR Global Positioning System, GPS, satellite geodesy,
08	05	--	space geodesy, radio positioning, radio interferometry

19 ABSTRACT (Continue on reverse if necessary and identify by block number)

The Global Positioning System (GPS) satellites transmit suppressed carrier signals which are modulated by pseudorandom "ranging" codes known as Coarse Acquisition (C/A) and Precise (P) codes. Range information can be derived by measuring the reconstructed carrier phase or the delay of the code modulation of a received signal. Subcentimeter level relative positioning has been achieved by measuring carrier phase. Improvements in relative positioning have been achieved by combining P code delay or "pseudorange" observations with phase observations. Since changes in the GPS will eventually make P code observations impossible for civilian users, this study examines the effect of combining C/A code observations with carrier phase observations. Carrier phase observations represent relatively precise, but biased, measurements of the satellite to receiver range. If phase observations are differenced between receivers and satellites, the bias is an integer number of cycles. If this integer value can be determined, position-determination accuracy is improved. Range measurements based on code delay may help to determine the integer bias. Unfortunately, the C/A code provides a relatively noisy range measurement.

In this study, C/A code observations were simulated using actual phase observations. The mean values of the ionospheric contributions to the simulated observations were determined from the International Reference Ionosphere (IRI) model, and variations about the means were derived from actual dual-frequency phase observations. These phase and C/A code observations were used to estimate biases and baseline vectors, for baseline lengths of 10, 100, and 330 km. The results of the simulation indicate that no significant improvement in positioning accuracy is obtained by adding C/A code to carrier phase observations. A possible explanation for the lack of improvement may be the assumption, in the analysis of the observations in this study, of zero a priori ionospheric contribution to the observations.

20. DISTRIBUTION / AVAILABILITY OF ABSTRACT ☐ UNCLASSIFIED/UNLIMITED ☒ SAME AS RPT ☐ DTIC USERS	21 ABSTRACT SECURITY CLASSIFICATION UNCLASSIFIED
22a NAME OF RESPONSIBLE INDIVIDUAL Dr. Thomas P. Rooney	22b TELEPHONE (Include Area Code) (617) 377-3486 — 22c OFFICE SYMBOL AFGL/LWG

DD FORM 1473, 84 MAR

83 APR edition may be used until exhausted
All other editions are obsolete

SECURITY CLASSIFICATION OF THIS PAGE

Contents

Figures

iv

Tables

Accession For	
NTIS GRA&I	☒
DTIC TAB	☐
Unannounced	☐
Justification	
By	
Distribution/	
Availability Codes	
Dist	Avail and/or Special
A-1	

1.0 Introduction

The Global Positioning System (GPS) has been used successfully for high precision relative positioning for nearly a decade.[1] The subcentimeter level accuracy achieved is attributed to the use of reconstructed carrier phase measurements of the signals received from GPS satellites. Additional improvements in accuracy have been obtained through the use of the Precise (P) code pseudorange information.[2,3] This improvement is significant if the observation period is short, making ambiguity resolution, without the P code delay observations, impossible. The lower accuracy Coarse/Acquisition (C/A) code has not been widely used together with phase observations. The purpose of this study is to evaluate the possible improvements in relative positioning which might result from addition of C/A code measurements to dual frequency phase observables. This work is motivated by changes which will take place when the new constellation of Block II satellites become active. All present work has been done using the aging constellation of Block I satellites. These satellites were designed to verify the accuracy of GPS positioning for defense applications, and to support development of GPS user equipment. This constellation consists of six operational satellites, in two orbital planes, oriented to provide maximum coverage over North America. In the Block I satellites none of the codes are encrypted. As the GPS system becomes operational with launching of the Block II satellites, the P code will be encrypted for national security reasons. The P code provides the highest accuracy, and unauthorized users possessing the code could use the knowledge to deceive authorized users. The introduction of advanced GPS receivers provides a second motivation for this study.

---

[1] Counselman III, C. C., et. al., "Accuracy of Baseline Determinations by MITES Assessed by Comparison with Tape, Theodolite, and Geodimeter Measurements", *EOS, the Transactions of the American Geophysical Union*, vol. 62, p. 260, April 28, 1981.

[2] Wubbena, G., A. Schuchardt, and G. Seeber, "Multistation positioning results with TI4100 GPS receivers in geodetic control networks", *Proc. Fourth International Geodetic Symposium on Satellite Positioning*, vol 2, pp 963-978, University of Texas, Austin, 1986

[3] Lichten, S.M., and J.S. Border, "Strategies for High-Precision Global Positioning System Orbit Determination", *Journal of Geophysical Research*, vol. 92, pp 12751-12762, 1987

Geodetic GPS receivers with the capability to measure precise dual frequency carrier phase as well as C/A code delay have been introduced. The Mini-Mac™ was the first receiver to enter the market. Several receivers with similar capabilities are also being marketed or have been announced.

The advantage of utilizing code delay information is that it is an unambiguous, relatively unbiased measurement of the satellite-receiver range. The carrier phase measurement is more precise, but contains a bias which must be determined to recover range information. The drawback of using delay, or pseudorange, information is the relatively large amount of noise present in it. A further disadvantage in using the C/A code is its availability at only a single frequency, making removal of the ionospheric delay difficult. It is hoped that by minimizing ionospheric contribution and noise, C/A code can enhance phase observations.

™Mini-Mac is a registered trademark of Aero Service Division, Western Geophysical Company of America.

2

2.0 Background material

This section will first describe the two types of GPS observables which are used for positioning. These observables are the phase and pseudorange measurements. Next, the errors which corrupt these measurements will be discussed.

2.1 GPS Signal Structure

The GPS satellites transmit positioning signals in two radio frequency bands, the L1 band and the L2 band, with carrier frequencies of 1575.42 MHz and 1227.60 MHz respectively. Both periodic carrier waves are phase modulated by pseudorandom codes. The codes appear as random noise to those not possessing the keys. Two different pseudorandom codes are used by the GPS system. A so-called Coarse/Acquisition (C/A) code modulates the L1 carrier. A second code, known at the Precise (P) code, modulates both carrier waves. As their names implies, the P code can provide greater positioning accuracy than the C/A code. The C/A code is used to acquire, or lock on to the GPS signals.[1] The modulation suppresses the carrier wave; however a carrier wave can be reconstructed. The wavelength of the carrier waves are 19 cm for L1 and 24 cm for L2. Range information can be derived by measurements of the reconstructed carrier phase and the code modulation delay.

2.2 Phase observable

The advantage of measuring the carrier phase is the precision with which the measurement can be made. Using a well designed antenna and receiver, the phase can be measured to one percent of a cycle, which corresponds to about 2 mm of range.

High accuracy relative positioning is readily obtained, using differenced phase measurements. In relative positioning the position of one station is known, and the position of the second station is determined with respect to the fixed station. The position solutions are

---

[1] Spilker, J. J., "GPS signal structure and performance characteristics", *Global Positioning System*, The Institute of Navigation, vol. 1, pp. 29-54, 1980.

generally not available in real time. Typically, observations taken over several hours are processed to determine baselines, with phase measurements typically taken every six minutes.

2.2.1 Codeless measurement

Several methods are available to measure the phase of the reconstructed carrier. If the receiver has knowledge of the modulating codes used by the GPS satellite, the carrier wave can be reconstructed. In this case the wavelengths of carrier are 19 cm and 24 cm, for the L1 and L2 bands respectively. This is the method used in the TI 4100 receiver in both L1 and L2 bands. If the receiver does not possess knowledge of the codes, the second harmonic of the incoming carrier is reconstructed. The codeless technique results in measurements made with a reconstructed carrier, having wavelengths of 9.5 cm and 12 cm respectively for the L1 and L2 bands. The shorter carrier wave observations are obtained from the Macrometer II™ at both L1 and L2 frequencies.[1] The Mini-Mac receiver is designed to use L1 code and no L2 code.[2]

2.2.2 Integer ambiguity

The one-way phase observable is a precise measurement of the fractional part of reconstructed carrier wave. Since this measurement is corrupted by errors, the unknown ambiguity is not an integer. By differencing observations between satellites and receivers, the errors are significantly reduced. The ambiguity parameter of the differenced observable is an integer. By determining the ambiguity parameter, uncertainties in positioning can be reduced. The process of resolving the ambiguity is known as bias fixing.

[™]Macrometer II is a registered trademark of Aero Service Division, Western Geophysical Company of America

[1]King, P.W., E.G. Masters, C. Rizos, A. Stolz, and J. Collins, *Surveying with GPS*, Monograph No. 9, School of Surveying, University of New South Wales, Kensington, N.S.W., Australia, November 1985

[2]Ladd, J.W., R.G. Welshe, "Mini Mac™ A New Generation Dual Band Surveyor", *Proc. Fourth International Geodetic Symposium on Satellite Positioning*, vol 2, pp 475-487, University of Texas, Austin, 1986.

2.3 Pseudorange observable

The second type of position information available is the time delay of the code modulation. The code observables serve to determine the unambiguous range of the satellites and to identify each satellite.

The satellite-receiver range is determined by measuring the time of the reception of the code modulated signal. The satellites transmit unique codes which are correlated with a replica, generated simultaneously in the receiver. The receiver code is delayed to maximize the correlation with the received signal. The added delay is a measure of the satellite-receiver range. This measured range is termed pseudorange, since it is corrupted by clock errors. If receiver and satellite clocks are synchronized, three satellites can accurately determine the receiver position in three dimensions. If receiver and satellite clocks are not synchronized, four satellites are needed. The redundant information is used to solve for relative receiver-satellite clock error.

The coded modulation makes them resistant to intentional and unintentional jamming. To prevent all the satellites from interfering with each other, the codes chosen have the property of being orthogonal to each other. Any cross correlation between any two codes will be zero, and only an autocorrelation results in a nonzero value. Different sections of the same code are also orthogonal to each other. This property is helpful against multipath propagation errors, as will be discussed in the section on errors.[1]

2.3.1 Coarse/Acquisition (C/A) Code

The C/A code occupies a bandwidth of approximately 1 MHz. The code consists of approximately 10^3 binary bits which is modulated at a rate of 1 Mbps, resulting in a duration of 1 msec per cycle of the C/A code. This code is used for acquiring the GPS signal and determining the satellite-receiver propagation delay. Information concerning clock correction, satellite ephemeris, and system messages also modulates the L1 carrier wave.[1]

---

[1] Spilker, J. J., GPS signal structure and performance characteristics", Global Positioning System, The Institute of Navigation, vol. 1, pp. 29-54, 1980.

The C/A code repeats itself eve.y millisecond, implying that the receiver and satellite clocks must be synchronized to within a millisecond, or the *a priori* receiver position must be known to within 300 km to determine unambiguous range measurements. A typical C/A code only receiver can determine position to within 30 m.

2.3.2   Precise (P) code

Unlike the C/A code, which will be available to everyone, the P code will be restricted to national security applications, when the Block II satelli~s are operational. The P code access is restricted to prevent the jamming of the GPS signals. A ground or satellite transmitter broadcasting the P code, near a receiver, will make accurate positioning impossible. The P code occupies a bandwidth of approximately 10 MHz. The total code length is 267 days, with each satellite assigned a unique one week segment of the code. Unlike the C/A code, the P code is broadcast on both the L1 and L2 bands, enabling the ionospheric effect to be reduced, and permitting higher accuracy. With the P code, three dimensional position can be determined to within 10 meters in real-time.[1]

2.4   Observation errors

Several factors contribute to degradation of both phase and pseudorange measurements, but to different degrees. These contributions are discussed in the following sections.

2.4.1   Oscillator phases

The largest source of error on one-way observables are the local oscillator phases, present in each satellite and receiver. These errors can be readily removed by differencing observations between receivers and satellites. Each of the GPS satellite is equipped with Cesium oscillators, where as the GPS receivers are equipped with relatively inexpensive, and less accurate, quartz oscillators. Both receiver and satellite oscillator phases will not permit the integer ambiguity to be determined, unless these errors are significantly reduced.

---

[1] Spilker, J. J., "GPS signal structure and performance characteristics", *Global Positioning System*. The Institute of Navigation, vol. 1, pp. 29-54, 1980)

6

2.4.2 Satellite Ephemeris

The inability to accurately predict the orbit of the GPS satellites, also limits the positioning accuracy. These error are also readily reduced by forming differences. The satellites are a finite distance form the receivers, and therefore the satellite ephemeris errors are passed onto baseline measurements. The difficulties in orbit prediction arise from the inability in accurately modeling all the forces acting on the satellites, and being unable tc precisely measure the initial conditions of the satellites. The ability to measure baselines, with fixed orbits, depends on the following empirical relationship:[1]

$$\frac{\text{baseline error}}{\text{baseline length}} = \frac{\text{orbit error}}{\text{height of satellite}}$$

With orbit errors of tens of meters and the height of GPS satellites at 20,183 km, the accuracy achievable is about one part in 10^7. To improve baseline accuracy, knowledge of the satellite orbits must be improved. It has been shown that the ability to fix biases on smaller baselines enhances the ability to determine orbits. Fixing biases on a baseline reduces the position uncertainty of the receivers, permitting higher accuracy orbit determination.[2]

2.4.3 Propagation delay

Significant error in range measurement is introduced by the environment, through which the GPS signals travel. One environmental error source is the ionospheric delay, whose effect is inversely proportional to the square of the frequency for code observables, and inversely proportional to frequency for phase observables. This property enables the the ionospheric contribution to be removed by making measurements at two frequencies and forming a linear combination of two measurements. This correction will discussed in more detail in Section 4.1. The ionosphere has different effects on the phase and

[1]Colombo, O.L., "Ephemeris Errors of GPS Satellites", *Bulletin Geodesique*, vol 60, pp 64-84, 1986.

[2]Abbot, R.I., C.C. Counselman III, and S.A. Gourevitch, "GPS Orbit Determination. Bootstrapping to Resolve Carrier Phase Ambiguity", presented at the *Fifth International Geodetic Symposium on Satellite Positioning*, New Mexico State University, Las Cruces, March 13-17, 1989.

pseudorange observables. The ionosphere advances the phase as the signal propagates through it, thereby decreasing the measured range to the satellite. The ionospheric delay for the pseudorange observable is opposite in sign to delay for the phase observable. The pseudorange observable is delayed by the ionosphere, resulting in larger range measurement. Ionospheric delay can range from several meters during the night to tens of meters during the day. The ionospheric delay is also dependent on solar activity, satellite elevation, and latitude of the GPS receiver. The ionospheric delay is large during periods of strong solar activity, low satellite elevations, and low latitudes. Another source of propagation error is the troposphere. Both water vapor and other dry atmospheric components further delay the GPS signals. Tropospheric delay can be readily modeled by using basic atmospheric measurements at the surface, such as temperature, pressure, and relative humidity. Unmodeled, the troposphere can produce errors on the order of tens of meters at low satellite elevations ($\approx 15°$). Using the three surface measurements, the tropospheric delay can be reduced to approximately 10 centimeters or less.[1]

2.4.4 Measurement errors

Two sources of error, which are functions of receiver and antenna design, excluding clocks, are thermal noise and multipath. Thermal noise in a well designed GPS receiver is limited to 1/2 % - 1 % of the wavelength of the carrier wave or the chipwidth of the codes.

Multipath propagation is the reflected signal which reaches the antenna via a path which is not the line of sight path. Reflected signals interfere with the direct signal, corrupting the measurements. The effect of multipath propagation has a different effect on each observable. With the use of a metallic, horizontal ground plane below the antenna elements, multipath effects on phase observations can be reduced to subcentimeter levels.[2] For the pseudorange

[1] Spilker, J. J., "GPS signal structure and performance characteristics", Global Positioning System, The Institute of Navigation, vol. 1, pp. 29-54, 1980

[2] Counselman III, C. C., S. A. Gourevitch, "Miniature Interferometer Terminals for Earth Surveying: Ambiguity and Multipath with Global Positioning System," IEEE Transactions on Geoscience and Remote Sensing, vol. GE 19, no. 4, pp. 244-252, October 1981

observable, the range error due to multipath propagation is limited to the chip width of the code being received. If the difference between the direct and reflected signal path is greater than one chip width, the receiver automatically rejects this signal due to the orthogonality property of the codes. On the other extreme is the case when the reflected signal path is approximately equal to the line of sight path. In this case the multipath effect is on the order 30 cm for P code.[2] Multipath propagation error is expected to be on the order of 1 m for one-way C/A code observations. This is the case for geodetic receivers, where the antenna is mounted 1-2 m above the ground. When the antenna is this close to the ground and stationary, multipath propagation errors exhibit quasiperiodic variations, due to the satellite's motion across the sky. The period of these variations is on the order of 15 minutes. This periodicity implies that a partial averaging of these errors occur over time.[1]

---

[1]Counselman III, C.C., personal communication (M I T).

3.0 Differencing observables

Oscillator phase, ionospheric, and tropospheric contributions must be significantly reduced to permit the integer ambiguity to be determined. These effects can be reduced by forming differences among a common set of observations, canceling common mode errors present in the observables.

3.1 Single Differencing

If two receivers simultaneously observe the same satellites, the observations from both receivers can be differenced. The new observable is known as a between receiver single difference observable. The geometry for single differencing is shown in Figure 3.1.
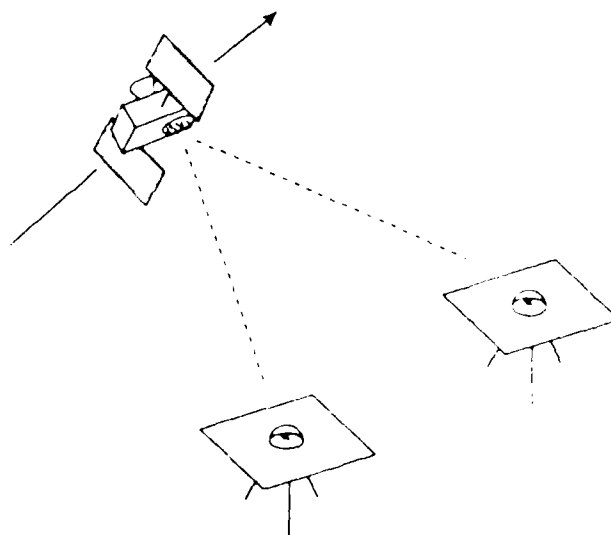

Figure 3.1 Satellite-receiver configuration for a single difference observable

In performing the single difference, the measured phase observations between the satellite and each receiver is differenced. In the process of being differenced, errors common to both range measurements cancel each other. This can be seen by forming a simplified theoretical equation

10

for a one-way observable. The phase that is measured at the receiver is a function of several factors shown in Equation 3.1. The notation used is from Footnote 1 given below.

$$\phi_k^i = \phi^i + \phi_k - \frac{1}{\lambda} r_k^i + n_k^i + \epsilon_k^i$$

(3.1)

i	- satellite index
k	- receiver index
ϕ_k^i	- measured phase of signal at receiver k from satellite i
ϕ^i	- satellite i oscillator phase
ϕ_k	- receiver k oscillator phase
λ	- wavelength of the reconstructed carrier signal
r_k^i	- actual range between receiver k and satellite i
n_k^i	- integer number of cycles between receiver k and satellite i at the initial epoch
ϵ_k^i	- errors in measured range
	- (i.e. ionosphere, troposphere, and satellite ephemeris)

The phase of the carrier signal increases as the range decreases, and decreases for increasing range, resulting in a negative sign in front of the range term. Using an additional one-way observable by a second receiver (q), a single difference observable can be formed:

$$\phi_k^i - \phi_q^i = \left(\phi^i + \phi_k \right) - \left(\phi^i + \phi_q \right) - \frac{1}{\lambda} \left(r_k^i - r_q^i \right) + \left(n_k^i - n_q^i \right) + \left(\epsilon_k^i - \epsilon_q^i \right)$$

(3.2)

q   - receiver index

Equation 3.2 can be simplified by denoting a single difference by (Δ):

[1] Beutler, G., et.al., "Using the Global Positioning System (GPS) for High Precision Geodetic Surveys: Highlights and Problem Areas", *IEEE PLANS '86 Positions Location and Navigation Symposium*, pp. 243-250, November 1986.

11

$$\Delta \phi^i_{kq} = \left(\phi_k - \phi_q \right) - \frac{1}{\lambda} \Delta r^i_{kq} + \Delta n^i_{kq} + \Delta \epsilon^i_{kq}$$

$$(3.3)$$

One of the primary benefits of single differencing is that satellite oscillator phases cancel. If the receivers are not widely separated, both the receivers essentially "see" the same ionosphere and troposphere; therefore, these errors are significantly reduced. The satellite ephemeris errors are also reduced. Reductions of the ionospheric contribution and the ephemeris errors are a function of baseline length.

3.2 Double Differencing

The procedure of differencing the observables can be expanded further, to cancel receiver oscillator phases. In the single difference observable, satellite oscillator phases cancel, but the difference of the two receiver oscillator phases remain. By adding a satellite to the scenario shown in Figure 3.1, a additional single difference observable can be formed. Both these differences do not contain satellite oscillator phases, but they do contain identical receiver oscillator phases. If one single difference, formed with satellite i, is differenced with another single difference, formed with satellite j, the resulting equation is shown below:

$$\Delta \phi^i_{kq} - \Delta \phi^j_{kq} = \left(\phi_k - \phi_q \right) - \left(\phi_k - \phi_q \right) - \frac{1}{\lambda} \left(\Delta r^i_{kq} - \Delta r^j_{kq} \right)$$
$$+ \left(\Delta n^i_{kq} - \Delta n^j_{kq} \right) + \left(\Delta \epsilon^i_{kq} - \Delta \epsilon^j_{kq} \right)$$

$$. (3.4)$$

$$j \qquad \text{- satellite index}$$

The receiver oscillator phases now cancel each other completely. The resulting observable is known as a double difference observable, and it contains no satellite or receiver oscillator

phases. If ($\Delta\Delta$) is used to d note a double difference quantity, Equation 3.4 can be simplified to:

$$\Delta\Delta\,\phi_{k\,q}^{i\,j} = -\frac{1}{\lambda}\,\Delta\Delta\,r_{k\,q}^{i\,j} + \Delta\Delta\,n_{k\,q}^{i\,j} + \Delta\Delta\,\epsilon_{k\,q}^{i\,j}$$

(3.5)

This configuration for forming a double difference observable is shown in Figure 3.2. Because the oscillator phases have been canceled, the double difference integer ambiguity parameter can be estimated as an integer. In practice, double difference observables are processed to estimate the integer ambiguity, and to determine the baselines between receivers.
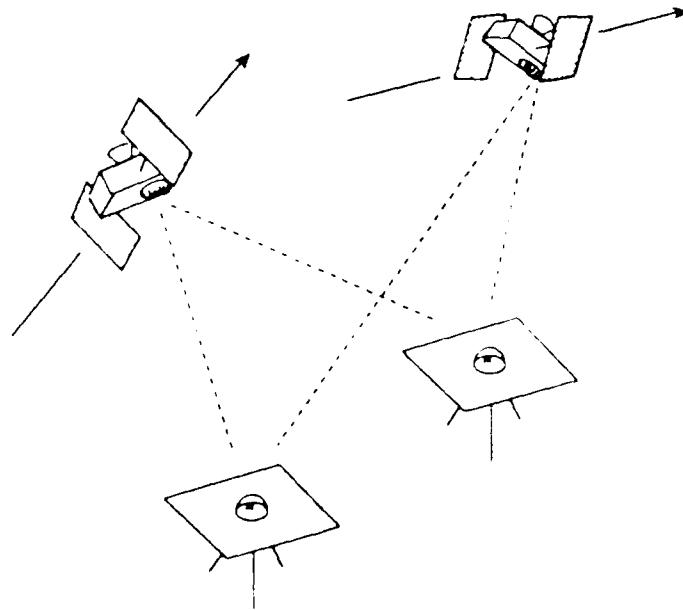

Figure 3.2 Satellite-receiver configuration for a double difference observable

Although the double differencing scheme is straightforward for two receivers and two satellites, it becomes more complicated when more than two satellites are involved. Earlier work involved picking one satellite as the reference satellite. This satellite was usually the first

13

satellite visible in the observing period. Observations from the remaining satellites would be differenced with the reference satellite. The drawback to this procedure was that the reference satellite appeared in the double differences more than the other satellites, and was given more weight in processing. More information was extracted from the reference satellite, than from the other satellites. With all the satellites having the same quality of orbits, it was incorrect to give more weight to one particular satellite.[1] This procedure for double differencing also results in observables, that no longer have independent errors. In forming linear combinations (i.e. forming differences) of the observables, the observable errors become correlated.

The solution to this problem of improper weighting, and to create uncorrelated observables is to orthogonalize the set of single differences formed at each epoch. This can be accomplished using Gram-Schmidt orthogonalization.[2] The general equation which forms equally weighted, independent double difference observables given a set of single differences at each epoch, using the notation previously developed is:[3]

$$
I\Delta\Delta\, \phi_{k\,q}^{i} = \sqrt{\frac{2\,i}{i+1}} \left[\Delta\,\phi_{k\,q}^{i+1} - \frac{1}{i}\sum_{m=1}^{i} \Delta\,\phi_{k\,q}^{m} \right].
\tag{3.6}
$$

$I\Delta\Delta$ - independent double difference observable

i - loops through 1 to (n - 1) satellites at each epoch

---

[1] Abbot, R.I., personal communication (M.I.T).

[2] Strang, G., *Linear Algebra and its Applications*, Academic Press, Inc., New York, NY, pp. 128-131, 1980.

[3] Remondi, B.W., "Using the Global Positioning System (GPS) phase observable for relative geodesy: modeling, processing, and results", *Ph.D Dissertation*, Center for Space Research, The University of Texas at Austin, 1984

4.0 Processing algorithm

The methods by which errors in the observables are reduced are discussed in Section 4.1. Later sections develop the normal equations, through which the observations are processed. Normal equations for L1 and L2 phase observables will be initially developed, and the same technique will be expanded to include the C/A code observable. Although the double difference notation ($\Delta\Delta$) is not used in this section, all the observations and parameters are double differenced before being processed.

4.1 Processing L1 and L2 observables

The integer ambiguity is estimated by first predicting the satellite-receiver range, using *a priori* station coordinates and integrated satellite ephemerides. From this predicted range, the expected phase observables are calculated and subtracted from the measured phases, to form the pre-fit residuals. If the theoretical model completely and accurately simulates reality, the prefit residuals will be zero. The model can than be used to determine the integer ambiguity. In practice, the prefit residuals are never zero. The prefit residuals are double differenced and processed through a maximum-likelihood estimation algorithm to estimate the integer ambiguity, the ionospheric contribution, and other parameters. The maximum likelihood function is given by Equation 4.1.

$$L(x_1,\ldots,x_n;\alpha) = \prod_1^n f(x_i;\alpha)$$

(4.1)

$f(\ )$ - frequency function
n - number of observables
x_i - independent random observations
α - unknown parameter

The function (f) is frequency function of known random variable x_i and unknown parameter α, which can be a function of several additional parameters. The likelihood function represents

15

the joint probability of observing the set of observations actually made. The goal is to determine α, which maximize the value of the likelihood function, given n observations (x_i). By maximizing the likelihood function, we are maximizing the probability that values of x_i observed are the most likely ones. If random observations have normal distributions, with mean of α and a standard variation of σ_i, the frequency function and the likelihood function can be written as shown below.

$$f(x_i ; \alpha) = \frac{1}{\sqrt{2\pi}\,\sigma_i}\ e^{-\frac{1}{2}\left(\frac{x_i - \alpha}{\sigma_i}\right)^2}$$

(4.2)

$$L(x_1, \ldots, x_n ; \alpha) = \frac{1}{(2\pi)^{\frac{n}{2}} \prod_1^n \sigma_i}\ e^{-\frac{1}{2}\sum_1^n \left(\frac{x_i - \alpha}{\sigma_i}\right)^2}$$

(4.3)

σ_i - assumed *a priori* standard deviation
for each observation

The exponent must be minimized to maximize the likelihood function. This exponent is the sum of the squares of the prefit residual, or chi-square (χ^2):

$$\chi^2 = \sum_1^n \left(\frac{x_i - \alpha}{\sigma_i}\right)^2$$

(4.4)

The goal is to determine which α minimizes χ^2, thereby maximizing L.[1]

If only L1 and L2 phase observables are used, the resulting χ^2 is shown below.

---

[1] Soiloway, C.B., *Elements of the Theory of Orbit Determination*, JPL Engineering Planning Document. No 225. December 1964.

16

$$\chi^2 = \sum_{i=1}^{Nepochs} \chi_i^2$$

$$(4.5)$$

$$\chi_i^2 = \frac{\left(\phi_{L1} - n_{L1} - d_{geom} - k\right)^2}{\sigma_{L1}^2} + \frac{\left(\phi_{L2} - n_{L2} - g\, d_{geom} - \frac{k}{g}\right)^2}{\sigma_{L2}^2}$$

$$(4.6)$$

ϕ_{L1} - L1 phase (L1 cycles)

ϕ_{L2} - L2 phase (L2 cycles)

g   - ratio of L2 and L1 frequencies

       - L2/L1 = 60/77

n_{L1} - L1 integer ambiguity

n_{L2} - L2 integer ambiguity

d_{geom} - satellite-receiver range in units of phase (L1 cycles)

       - includes atmospheric contribution

       - function of several parameters

k   - theoretical ionospheric phase at L1 frequency

       - assumed independent, for every epoch and

         satellite-receiver combination (L1 cycles)

σ_{L1} - assumed *a priori* standard deviation

       for L1 phase observable (L1 cycles)

σ_{L2} - assumed *a priori* standard deviation

       for L2 phase observable (L2 cycles)

Using the notation developed in Section 3.1, d_{geom} can be defined as:

$$d_{geom} = \frac{1}{\lambda}\, r_k^i$$

$$(4.6a)$$

By minimizing χ^2 with respect to the ionosphere (k) and geometry parameters (d_{geom}), the value of the parameters are given below.

17

$$k = \frac{g}{1-g^2} \left(\phi_{L2} - g\, \phi_{L1} \right) \tag{4.7}$$

$$d_{geom} = \frac{1}{1-g^2} \left(\phi_{L1} - g\, \phi_{L2} \right) \tag{4.8}$$

Both parameters of linear combinations of the L1 and L2 observables. The integer bias parameters (n_{L1} and n_{L2}) have been absorbed into its respective phase observable (i.e. $\phi'_{L1} = \phi_{L1} - n_{L1}$). The expression for the ionosphere (k) is known as the geometry-free observable, since it contains no geometrical, or range, information. Equation 4.8 is known as the "LC" observable, and is free of ionospheric effects. It is shown below.

$$\phi_{LC} = \phi'_{L1} - \frac{g}{1-g^2} \left(\phi'_{L2} - g\, \phi'_{L1} \right)$$

$$= \phi'_{L1} - k \tag{4.9}$$

$$\phi'_{L1} = \phi_{L1} - n_{L1} \tag{4.9a}$$

$$\phi_{LC} \quad \text{- ionosphere-free phase observable (L1 cycles)}$$

Equation 4.9 shows that the expression for d_{geom} is the L1 phase observable with the ionosphere removed.

Instead of using the LC observable, an alternative approach is taken to permit the phase cycle ambiguity to remain an integer. This method was developed by Dr. Sergei Gourevitch at

MIT. Chi-square is rewritten to include a constraint on the ionospheric contribution. Equation 4.6 can be rewritten as shown below.

$$\chi_i^2 = \frac{\left(d_{ion} - k\right)^2}{\sigma_{ion}^2} + \frac{\left(\phi_{L1} - n_{L1} - d_{geom} - k\right)^2}{\sigma_{L1}^2}$$

$$+ \frac{\left(\phi_{L2} - n_{L2} - g\,d_{geom} - \frac{k}{g}\right)^2}{\sigma_{L2}^2}$$

(4.10)

d_{ion} - theoretical ionospheric contribution to the L1 carrier phase (L1 cycles)

   - average value of the ionosphere

σ_{ion} - assumed *a priori* standard deviation for the ionospheric contribution (L1 cycles)

   - ionospheric constraint

It is now clear that Equation 4.6 is a special case of Equation 4.10, when σ_{ion} approaches infinity. On the other extreme is the case when σ_{ion} approaches zero, implying that the ionospheric contribution is accurately known, and the L1 and L2 observables are processed independently. If no *a priori* value for the ionosphere is available than d_{ion} is set to zero. A ionosphere model was not used determine d_{ion} in this study, and it was assumed to be zero. The ionosphere (k) in Equation 4.10 is removed implicitly, for every epoch and satellite-receiver combination. This is accomplished by minimizing χ^2 with respect to k, and substituting the expression for k back into χ^2. In doing this, the value of the ionosphere is being estimated using L1 and L2 phase observables. The ionosphere (k) is implicitly determined to reduce the number of parameters that are solved for in the normal equations.

The process of forming the normal equations from Equation 4.10 will now be discussed. The goal is rewrite χ^2 in a quadratic form, from which the normal equations can be readily derived. The quadratic form is shown below.

$$\chi_i^2 = [V]^T[W][V] \tag{4.11}$$

$$[V] = \begin{bmatrix} d_{geom} \\ d_{ion} \end{bmatrix} - \begin{bmatrix} \phi_{geom} \\ \phi_{ion} \end{bmatrix} \tag{4.12}$$

ϕ_{geom} - ionosphere-free observable

ϑ_{ion} - geometry-free observable

The weight matrix $[W]$ contains information on the *a priori* errors in the L1 and L2 phase observables and the ionosphere.

$$[W] = \begin{bmatrix} w_{11} & w_{12} \\ w_{21} & w_{22} \end{bmatrix} \tag{4.13}$$

$$\begin{bmatrix} \phi_{geom} \\ \phi_{ion} \end{bmatrix} = [T] \begin{bmatrix} \phi_{L1} \\ \phi_{L2} \end{bmatrix} \tag{4.14}$$

The transformation matrix $[T]$ transforms L1 and L2 observables to ionosphere-free and geome y-free observables.

$$[T] = \begin{bmatrix} t_{11} & t_{12} \\ t_{21} & t_{22} \end{bmatrix} \tag{4.15}$$

Finally χ^2 can be fully expanded:

$$\chi_i^2 = \left[\begin{bmatrix} d_{geom} \\ d_{ion} \end{bmatrix} - \begin{bmatrix} t_{11} & t_{12} \\ t_{21} & t_{22} \end{bmatrix} \begin{bmatrix} \phi_{L1} \\ \phi_{L2} \end{bmatrix} \right]^T \begin{bmatrix} w_{11} & w_{12} \\ w_{21} & w_{22} \end{bmatrix} \left[\begin{bmatrix} d_{geom} \\ d_{ion} \end{bmatrix} - \begin{bmatrix} t_{11} & t_{12} \\ t_{21} & t_{22} \end{bmatrix} \begin{bmatrix} \phi_{L1} \\ \phi_{L2} \end{bmatrix} \right]$$

(4.16)

The terms in the weight and the transformation matrix were determined by equating Equation 4.16 with Equation 4.10, with the ionosphere term (k) implicitly solved for. The appropriate partial derivatives were taken of both sides, isolating the desired element in each matrix:

$$t_{i,j} = \frac{1}{2} \frac{\partial^2 \left(\chi_i^2 \right)}{\partial (d_i) \partial (\phi_j)}$$

(4.17)

$$w_{i,j} = \frac{1}{2} \frac{\partial^2 \left(\chi_i^2 \right)}{\partial (d_i) \partial (d_j)}$$

(4.18)

where,

$$\phi_1 = \phi_{L1} \qquad\qquad d_1 = d_{geom}$$
$$\phi_2 = \phi_{L2} \qquad\qquad d_2 = d_{ion}$$

The one half term accounts for the factor two which results from taking a derivative of a quadratic term. Only the subscript i on Chi-square (χ^2) represents the ith epoch. These calculations were carried out by Dr. Gourevitch, using Macsyma. The full expressions for the transformation and weight matrices are given in Appendix A. By examining the transformation matrix, its clear that the transformed observables are the same geometry-free and ionosphere-free observables developed in the previous example. The new observables are a simple rotation of the old observation vector. Since the observables are processed using linearized least squares, the geometrical and the ionosphere models are calculated about a *a priori* value.

21

$$d_{geom} = \left(d_{geom} \right)_o + \sum_{i=1}^{n} \frac{\partial d_{geom}}{\partial x_i} x_i$$

(4.19)

$$d_{ion} = \left(d_{ion} \right)_o + \sum_{i=1}^{n} \frac{\partial d_{ion}}{\partial y_i} y_i$$

(4.20)

$(d_{geom})_o$	- *a priori* value of satellite range (L1 cycles)
$(d_{ion})_o$	- *a priori* value of the ionospheric contribution (L1 cycles)
x_i	- geometrical parameters
y_i	- ionosphere parameters (L1 cycles)

.

The observables are replaced by its residuals as shown below.

$$\phi_{L1} = \phi_{L1} - \left(d_{geom} \right)_o$$

(4.21)

$$\phi_{L2} = \phi_{L2} - g \left(d_{geom} \right)_o$$

(4.22)

The geometry, or range model, and the ionosphere model are replaced by its variations about the *a priori* value.

$$d_{geom} = \sum_{i=1}^{n} \frac{\partial d_{geom}}{\partial x_i} x_i$$

(4.23)

$$d_{ion} = \sum_{i=1}^{n} \frac{\partial d_{ion}}{\partial y_i} y_i$$

(4.24)

If an *a priori* ionospheric contribution is also removed from the prefit phase residuals, then the parameter k gets replaced by

$$k = k - \left(d_{ion} \right)_o .$$

The next step is to further expand χ^2 and to form the normal equations for least squares analysis. Reinserting the biases, matrix $[V]$ becomes

$$[V] = \begin{bmatrix} d_{geom} \\ d_{ion} \end{bmatrix} - [T] \begin{bmatrix} \phi_{L1} - n_{L1} \\ \phi_{L2} - n_{L2} \end{bmatrix} .$$

The bias parameter, like the other geometric parameters, can be rewritten as

$$n_{L1} = \sum_{i=1}^{n} \frac{\partial d_{geom}}{\partial (n_{L1})_i} (n_{L1})_i$$

$$n_{L2} = \sum_{i=1}^{n} \frac{\partial d_{geom}}{\partial (n_{L2})_i} (n_{L2})_i$$

Now $[V]$ can be rewritten with explicit partials.

$$[V] = \begin{bmatrix} \dfrac{\partial d_{geom}}{\partial x} x + t_{11} \dfrac{\partial d_{geom}}{\partial n_{L1}} n_{L1} + t_{12} \dfrac{\partial d_{geom}}{\partial n_{L2}} n_{L2} \\ \dfrac{\partial d_{ion}}{\partial y} y + t_{21} \dfrac{\partial d_{geom}}{\partial n_{L1}} n_{L1} + t_{22} \dfrac{\partial d_{geom}}{\partial n_{L2}} n_{L2} \end{bmatrix} - \begin{bmatrix} \phi_{geom} \\ \phi_{ion} \end{bmatrix}$$

It should be noted that the parameters (x, y, n_{L1}, n_{L2}) above represent a vector; therefore, the partial derivatives also represent vectors.

$$\frac{\partial\, d_{geom}}{\partial\, n_{L1}} = \left[\begin{array}{ccc} \dfrac{\partial\, d_{geom}}{\partial\, (n_{L1})_1} & \dfrac{\partial\, d_{geom}}{\partial\, (n_{L1})_2} & \cdots \end{array} \right] \tag{4.30}$$

$$n_{L1} = \left[\begin{array}{c} (n_{L1})_1 \\ \\ (n_{L1})_2 \\ \cdot \\ \cdot \\ \cdot \end{array} \right] \tag{4.31}$$

In practice, the L2 phase ambiguity parameters are not directly solved for. The phase ambiguity of the beat frequency of L1 and L2 signals is calculated. The beat frequency of approximately 350 MHz is obtained by differencing the two carrier frequencies. The wavelength of this beat frequency is 86 cm, and for codeless receivers the wavelength is reduced to 43 cm. This bias known as the wide lane bias.[3] It is determined by differencing the L1 and L2 bias parameters. In Equation 4.29 the n_{L2} bias is replaced by the wide lane bias ($n_{L2} - n_{L1}$). This requires that the elements of the transformation matrix in Equation 4.29, and only this equation, be replaced by the following expressions:

$$t_{11} = t_{11} + t_{12} \tag{4.32}$$
$$t_{21} = t_{21} + t_{22} \tag{4.33}$$

Equation 4.29 can be further simplified to:

$$[V] = \begin{bmatrix} \dfrac{\partial\, d_{geom}}{\partial\, x} & 0 & t_{11}\dfrac{\partial\, d_{geom}}{\partial\, n_{L1}} & t_{12}\dfrac{\partial\, d_{geom}}{\partial\, n_{L2}} \\[2ex] 0 & \dfrac{\partial\, d_{ion}}{\partial\, y} & t_{21}\dfrac{\partial\, d_{geom}}{\partial\, n_{L1}} & t_{22}\dfrac{\partial\, d_{geom}}{\partial\, n_{L2}} \end{bmatrix} \begin{bmatrix} x \\ y \\ n_{L1} \\ n_{L2} \end{bmatrix} - \begin{bmatrix} \phi_{geom} \\ \phi_{ion} \end{bmatrix}$$

. (4.34)

or in a more compact notation:

$$[V] = [P]\, z - \phi_t .$$
(4.35)

$[P]$ - partial derivative matrix

z - parameter vector

ϕ_t - transformed observation vector

Reinserting [V] back into Equation 4.11, and expanding we get:

$$\chi_i^2 = z^T[P]^T[W][P]\, z - 2\, z^T[P]^T[W]\, \phi_t - \phi_t^T[W]\, \phi_t .$$
(4.36)

Now, χ^2 can be easily minimized with respect to the adjustable parameters (z). This is accomplished by taking the partial derivative of Equation 4.36 with respect to z, and setting the equation to zero. The resulting set of linear equations are known as the normal equations, and are solved for z.

$$[A]\, z = [B]$$
(4.37)

$$[A] = \sum_{i=1}^{Nepochs} [P]^T[W][P]$$
(4.38)

25

$$[B] = \sum_{i=1}^{Nepochs} [P]^T [W] \, \phi_i$$

(4.39)

$$z = \begin{bmatrix} x \\ y \\ n_{L1} \\ n_{L2} \end{bmatrix}$$

(4.40)

Success of this approach depends on the accuracy of the constraint placed on the ionosphere. The effect of the ionospheric contribution are inseparable from the integer ambiguity. To get accurate integer bias values, the ionosphere must be accurately constrained. If the ionospheric constraint (σ_{ion}) is small, the ionospheric parameters cannot be sufficiently adjusted to agree with the observations. If the ionospheric constraint is too large, the uncertainty is passed onto the estimates of the bias parameters and it becomes difficult to fix biases.

4.2 Addition of the C/A code

This concept of estimating ionospheric parameters can be extended to include pseudorange observables, in particular the C/A code. Although the pseudorange observable is noisy and imprecise, it contains unambiguous range information, which is not available with phase observable. A simple example can show the advantages of adding pseudorange information. This example looks at the effect of combining pseudorange and phase observables, with the ionosphere effects neglected. Chi-squared is written as:

$$\chi^2 = \sum_{i=1}^{Nepochs} \chi_i^2$$

(4.41)

26

$$\chi_i^2 = \frac{\left(\phi_{C/A} - d_{geom}\right)^2}{\sigma_{C/A}^2} + \frac{\left(\phi_{L1} - n_{L1} - d_{geom}\right)^2}{\sigma_{L1}^2} \quad . \tag{4.42}$$

$\phi_{C/A}$ - C/A code observable (L1 cycles)

$\sigma_{C/A}$ - assumed *a priori* standard deviation for
the C/A code observable (L1 cycles)

For this study C/A code observations have been converted from units of delay to phase.
Minimizing χ^2 with respect to geometry (d_{geom}) and bias (n_{L1}) parameters, and making use of
Equations 4.23 and 4.27, the normal equation can be written as:

$$\sum_{i=1}^{Nepochs} \left\{ [A] \begin{bmatrix} x \\ n_{L1} \end{bmatrix} = [B] \right\} \tag{4.43}$$

$$[A] = \begin{bmatrix} \left(\frac{\partial d_{geom}}{\partial x}\right)^2 \left(\frac{1}{\sigma_{C/A}^2} + \frac{1}{\sigma_{L1}^2}\right) & \left(\frac{\partial d_{geom}}{\partial x}\right)\left(\frac{\partial d_{geom}}{\partial n_{L1}}\right)\frac{1}{\sigma_{L1}^2} \\ \left(\frac{\partial d_{geom}}{\partial x}\right)\left(\frac{\partial d_{geom}}{\partial n_{L1}}\right)\frac{1}{\sigma_{L1}^2} & \left(\frac{\partial d_{geom}}{\partial n_{L1}}\right)^2 \frac{1}{\sigma_{L1}^2} \end{bmatrix} \tag{4.44}$$

$$[B] = \begin{bmatrix} \frac{\partial d_{geom}}{\partial x}\left(\frac{\phi_{C/A}}{\sigma_{C/A}^2} + \frac{\phi_{L1}}{\sigma_{L1}^2}\right) \\ \frac{\partial d_{geom}}{\partial n_{L1}}\left(\frac{\phi_{L1}}{\sigma_{L1}^2}\right) \end{bmatrix} \tag{4.45}$$

By taking the inverse of [A], we get a covariance matrix of errors for the parameters. In this example the covariance matrix contains elements which are the inverse of elements in matrix [A]. The magnitude of elements in the covariance matrix can be reduced by decreasing σ_{L1} or by introducing a nonzero $\sigma_{C/A}$. The value of covariance matrix elements can also be reduced by decreasing $\sigma_{C/A}$. The analysis shows that for a given geometry (i.e. the partials are the same), the C/A code or other pseudorange information will help reduce the uncertainty in the estimate of the bias. If the pseudorange information is very noisy (large $\sigma_{C/A}$), the improvement is negligible.

The approach used in Section 4.1 can expanded to include an additional type of observable. In this study, the aim is to add the ability to process C/A code observables along with the two phase observables. First, χ^2 must be reformulated to include the residual of the C/A observable:

$$\chi_i^2 = \frac{\left(d_{ion} - k\right)^2}{\sigma_{ion}^2} + \frac{\left(\phi_{L1} - n_{L1} - d_{geom} - k\right)^2}{\sigma_{L1}^2}$$

$$+ \frac{\left(\phi_{L2} - n_{L2} - g\, d_{geom} - \frac{k}{g}\right)^2}{\sigma_{L2}^2} + \frac{\left(\phi_{C/A} - d_{geom} + k\right)^2}{\sigma_{C/A}^2} \qquad (4.46)$$

The ionosphere contribution term (k) is eliminated as previously described. The difference now is that there are three observables, and we need to transform them into two observables. The transformation becomes a fit of three observable to the desired two observables, instead of a simple rotation, or linear combination, of just two observables. To account for any differences in χ^2 between the form in Equation 4.46 and the quadratic form, an additional term (c) is introduced as shown below:

$$\chi_i^2 = [V]^T [W][V] + c \tag{4.47}$$

c   - term to account for difference in χ^2 between
Equations 4.46 and 4.47

Now the transformed observables are determined as follows:

$$
\begin{bmatrix} \phi_{geom} \\ \phi_{ion} \end{bmatrix} = \begin{bmatrix} t_{11} & t_{12} & t_{32} \\ t_{21} & t_{22} & t_{32} \end{bmatrix} \begin{bmatrix} \phi_{L1} \\ \phi_{L2} \\ \phi_{C/A} \end{bmatrix} \tag{4.48}
$$

Since the quantities being fitted are observables, the resulting discrepancy (c) between the two forms of χ^2 will again only be a function of the observables. None of the parameters will be involved, implying that when χ^2 is minimized with respect to the parameters, the additional term (c) will not affect the normal equations. The weight and transformation matrices are calculated as described in Section 4.1. All the terms are reinserted into Equation 4.47, which is then subtracted from Equation 4.46, and extra term (c) can now be determined. As before, if the wide lane biases ($n_{L2} - n_{L1}$) are desired, Equations 4.32 and 4.33 must be substituted into Equation 4.34. These calculations were also carried out by Dr. Gourevitch using Macsyma. Complete expressions for the weight and transformation matrices, and the term (c) is given in Appendix B. By setting the weight ($1/\sigma_{C/A}^2$) for the C/A code to zero, it is apparent that the L1 and L2 only case is a subset of this formulation. The term (c) is zero if the weight for any observable is zero.

The normal equations are formed as describe in Section 4.1 and used to solve for the bias parameters. The C/A code not only provides range information, but also information on the ionospheric contribution. The sign for ionospheric contribution is different for the phase

and pseudorange observables since the ionosphere advances the phase of the carrier wave, but retards the code modulation.

4.3   Simulation of C/A code observable

To study the effect of the processing C/A code and phase observations, C/A code observations were simulated and processed with real phase observation. The details of forming C/A observations are discussed in this section.

Several error sources corrupt the measurements of pseudorange observations. The two major sources of error are the ionosphere and multipath. The C/A code observables were created by modifying real L1 phase observable in two steps. First, the position of one station on the baseline was adjusted using the LC observable. Since this observable was free of ionospheric contributions, the resulting position adjustment was also free of ionospheric effects. The adjusted position was then used to calculate the theoretical range to the satellites. This updated theoretical range was used to form the prefit residuals, which were used to simulate the C/A code observations.

The ionosphere-free position adjustment was used to form the L1 and L2 phase residuals. These residual were then used to form a LC observable, as shown in Equation 4.9. The C/A code was formed as shown below:

$$\phi_{C/A} = 2\,\phi_{LC} - \phi_{L1} + \text{(ionospheric contribution bias)} + \text{(noise)} \qquad (4.49)$$

$$= \phi_{L1} - 2\,\frac{g}{1-g^2}\left(\phi_{L2} - g\,\phi_{L1}\right)$$
$$+ \text{(ionospheric contribution bias)} + \text{(noise)} \qquad (4.50)$$

The ionospheric contribution was simulated by the measuring the change in the ionospheric contribution relative to the first epoch, using L1 and L2 phase measurements. The resulting

ionosphere in the C/A code observable has the opposite sign than the ionospheric contribution in the phase observables. The International Reference Ionosphere (IRI) Model was used to determine the mean value of the ionospheric contribution. This model is capable of predicting spatial and temporal variations within the ionosphere.[1] There are two ways in which the model can be utilized to calculate the constant term. The first method is to compute, from the IRI model, the ionospheric delay at the first epoch, in each series of observations. The second method involves determining the constant term at every epoch, by subtracting the (L2 - g L1) term from the value determined from the model, and than calculating the average value of this constant over the entire series. The first method was used in this study to determine the constant value.

The second major source of error contaminating the C/A code observable is multipath. As stated in Section 2.4.4, multipath propagation errors exhibit a period of approximately 15 minutes. This period is slightly more than twice the observation interval of 7 minutes. This fact allows the correlation between successive observations to neglected, and permits each observation to have independent statistics. For this study the double difference C/A code observations were assumed to have uncorrelated gaussian noise of 2 m rms. The one-way C/A code observations were modeled with 1 m of random gaussian noise. In forming differences, the variances of one-way noise terms add, increasing the noise present on double difference observables.

The receiver system noise (kT) was considered negligible. Tropospheric contribution was also considered negligible for this study.

The value of chi-square per degree of freedom, or reduced chi-square (χ_v^2), was used to adjust the assumed *a priori* measurement errors for the phase observables and the

---

[1] Rawer, K., D. Bilitza, "Study of Ionospheric and Tropospheric Models", NASA Report N86 26750, 1985.

ionosphere, to assure that they are properly weighted relative to the C/A code. Chi-square can also be written in terms of estimated and assumed *a priori* measurement errors.[1]

$$\chi^2 = \frac{s^2}{\bar{\sigma}^2} \nu \qquad (4.51)$$

$$\bar{\sigma}^2 = \frac{1}{N_{observations}} \sum_{i=1}^{N_{observations}} \sigma_i^2 \qquad (4.52)$$

$$\nu = N_{observations} - N_{parameters} - 1 \qquad (4.53)$$

s - estimated measurement error

$\bar{\sigma}^2$ - average assumed a priori measurement error

ν - number of degrees of freedom

The reduced chi-square (χ_ν^2) can be defined as:

$$\chi_\nu^2 = \frac{\chi^2}{\nu} = \frac{s^2}{\bar{\sigma}^2} \qquad (4.54)$$

χ_ν^2 - chi-square per degree of freedom

If the estimated measurement errors accurately represent the *a priori* measurement errors, the value χ_ν^2 is approximately 1. If the *a priori* errors resulted in χ_ν^2 not equal to one, these *a priori* errors (σ_i) were scaled,

---

[1]Bevington, P R , *Data Reduction and Error Analysis for the Physical Sciences*, McGraw-Hill Book Co ,New York, NY, pp. 187-189, 1969.

$$\sigma_s^2 = \frac{\sigma_i^2}{\chi_v^2} \quad , \tag{4.55}$$

σ_i - initial assumed *a priori* measurement error

σ_s - scaled assumed *a priori* measurement error

forcing χ_v^2 to equal one. The *a priori* error for the ionosphere was also scaled to preserve the relative weighting of the phase observables and the ionosphere. Since the error in the C/A code was simulated, its *a priori* measurement error was accurately known. Phase and ionospheric contribution *a priori* errors were scaled to assure that the relative weighting of the phase observables, C/A code observables, and the ionospheric delay were consistent.

L1 and L2 phase observations, recorded November 8, 1988 in east Texas, were used to form C/A code observations. Observations for baseline lengths ranging from 10 km to 330 km were recorded. For this study, observations from 10 km, 100 km, and 330 km baselines were processed. The initial *a priori* measurement and ionosphere uncertainties were based on previous analysis of this data.[1] The observations were processed for single baselines. The simulated C/A code observations were processed with the phase observables, having scaled *a priori* errors. To keep the analysis simple, only one station position and the L1 and L2-L1 bias parameters were solved for. These results were compared to solutions performed without the C/A code.

---

[1] Abbot, R.I., C.C. Counselman III, and S.A. Gourevitch, "GPS Orbit Determination: Bootstrapping to Resolve Carrier Phase Ambiguity", Presented at the *Fifth International Geodetic Symposium on Satellite Positioning*, New Mexico State University, Las Cruces, March 13-17, 1989.

5.0 Results

This section presents test results which establish the validity of the compute· programs, and show the effect of combining C/A code observations with L1 and L2 phase observations. First the validity of the program was established, using simulated L1 phase, L2 phase, and C/A code observations. After verification of the programs, simulated C/A code observations were processed with real phase observations.

5.1 Verification of programs

Upon completion of modifications to the software, the computer programs were tested using two separate procedures. No ionospheric effect was modeled for the simulated observations. The *a priori* ionospheric parameter (k) assumed to have a zero mean. It was not fixed. and allowed to vary with with a standard deviation of 0.001 ppm. A set of simulated observations were created, and processed through the least squares algorithm. In the simulated observations, noise was added by using gaussian random number generator. The noise for the double difference phase observations had a zero mean, with a standard deviation of approximately 0.2 L1 cycle of phase, or an equivalent path length of 2 cm. The noise for the double difference C/A code observations also had a zero mean, with a standard deviation of approximately 20 L1 cycles of phase, or an equivalent path length of 2 m. The prefit residual for each observable was simulated. The prefit residuals were simulated for two baselines: a 10 km baseline and a 100 km baseline. The simulations were based on a actual observation schedule. In processing the simulated observations, 13 parameters were adjusted: 3 station coordinates, 5 L1 bias parameters, and 5 L2-L1 (wide lane) bias parameters.

The equations were initially checked for consistency. The assumed *a priori* standard deviation of the observations must be consistent with the standard deviation of the simulated random noise. This check was accomplished by looking at value of Chi-square per degree of freedom (χ_v^2). If the equations are correct, and consistent weights are used, the value for Chi-square per degree of freedom should be approximately one.

Since the simulated errors of observations were noise with zero mean, the adjustments to the parameters should also be random variables with zero mean. The uncertainty of the adjusted parameters will also be random variables. Several factors influence the parameter adjustments. Averaging of many observations reduces the size of adjustments. The geometry of the satellite spacing in the sky, tends to increase the parameter adjustments, since in general the satellites are not evenly distributed across the sky.

For each baseline the observations were processed in two groups. First the L1 and L2 phase residuals were processed, and then C/A code residuals were added and processed. The results for the 10 km baseline are given in Table 5.1. The uncertainties given below are defined as three times the formal standard deviation of error of the related parameters and is multiplied by χ_v^2.

The adjustment of the position coordinates and the L1 bias parameters are zero to within a few millimeters. The uncertainty for the station coordinates and the L1 bias parameters are on the order of 1 cm, which was the assumed *a priori* standard deviation of the observations. The uncertainty in the L2-L1 bias is on the order of 5 cm. The L2-L1 bias uncertainty is greater than that for the L1 bias, since it is a linear combination of the uncertainties in the L1 and L2 bias. It was assumed that the observations were from a codeless receiver. The wavelength of the simulated L1 cycle phase corresponds to 1/2 L1 phase, and the simulated L2-L1 cycle phase corresponds to 1/2 (L2-L1) phase. A phase change of 1 cycle at L1 frequency and L2-L1 beat frequency is equivalent to a change in path length of 9.5 cm and 43 cm respectively. Similar results were obtained for the 100 km baseline, and are not presented here.

Table 5.1 10 km baseline parameter adjustments and uncertainties

Parameters	L1 + L2		L1 + L2 + C/A	
	Adjustment	Uncertainty $(3*\sigma_{uncertainty}*\chi_v^2)$	Adjustment	Uncertainty $(3*\sigma_{uncertainty}*\chi_v^2)$
χ_v^2	0.926		0.903	
Latitude (rad)	0.143×10^{-7}	0.49×10^{-7} (0.005m)	0.143×10^{-7}	0.53×10^{-7} (0.005m)
Longitude (rad)	0.186×10^{-7}	0.14×10^{-6} (0.013m)	0.189×10^{-7}	0.53×10^{-6} (0.013m)
Radius (km)	-0.116×10^{-5}	0.12×10^{-4} (0.012m)	-0.113×10^{-5}	0.53×10^{-4} (0.012m)
L1 Bias (L1 cycles):				
1	-0.0439	0.101	-0.0443	0.0995
2	-0.0322	0.115	-0.0327	0.114
3	-0.0587	0.113	-0.0588	0.112
4	-0.0032	0.120	-0.0041	0.118
5	-0.0611	0.169	-0.0594	0.167
L2-L1 Bias (L2-L1 cycles):				
1	0.0531	0.120	0.0538	0.119
2	0.0240	0.126	0.0248	0.124
3	0.0802	0.130	0.0807	0.128
4	0.0587	0.119	0.0603	0.117
5	0.0849	0.138	0.0824	0.137

5.2 Integer ambiguity determination

Next, the effect of including C/A code observables on the uncertainties in the estimation of station position coordinates and the bias parameters was studied. Observations for a given baseline were processed with and without the simulated C/A code observations. The a priori standard deviation of double difference phase observations and the ionosphere are listed in Table 5.2. The standard deviation was calculated by taking the constant term and adding a second term, that is proportional to baseline length.

Table 5.2 Assumed a *priori* standard deviation of double difference observations

	Constant term	Distance proportional term
Phase observations	3.5 mm	1.0 ppm
Ionospheric contribution	0.0 mm	30.0 ppm

Observations for 10 km, 100 km, and 330 km baselines were processed. On the 10 km baseline, the addition of C/A code observations resulted in a slight increase in the uncertainty of the parameter estimate, as shown in Table 5.3. In both cases the uncertainty of the bias parameters were small enough to enable these parameters to be fixed to an integer value, using the method described in Footnote 1 given below.

One possible explanation for results shown in Table 5.3 is the erroneous assumption of zero *a priori* ionospheric contribution on both the phase and pseudorange observables. This assumption was implicitly made by setting d_{ion} to zero (see Section 4.1). The ionospheric effect (k) on L1 double difference observable was also assumed to be an independent random variable with zero mean and a standard deviation (σ_{ion}) which was a function of baseline length. In reality the observations contain a non-zero *a priori* ionospheric contribution, which is correlated in time. This systematic error was also present in the C/A code; therefore, by adding pseudorange observations to phase observations the parameter estimates are further corrupted.

Table 5.3 10 km baseline uncertainties in parameter estimates

Parameters	L1 + L2 Uncertainty $(3*\sigma_{uncertainty}*\chi_v^2)$	L1 + L2 + C/A Uncertainty $(3*\sigma_{uncertainty}*\chi_v^2)$
Latitude (rad)	0.31×10^{-7} (0.003m)	0.32×10^{-7} (0.004m)
Longitude (rad)	0.86×10^{-7} (0.008m)	0.88×10^{-7} (0.009m)
Radius (km)	0.78×10^{-5} (0.008m)	0.80×10^{-5} (0.008m)
L1 Bias (L1 cycles):		
1	0.407	0.414
2	0.425	0.433
3	0.439	0.447
4	0.401	0.408
5	0.465	0.474
L2-L1 Bias (L2-L1 cycles):		
1	0.117	0.119
2	0.122	0.124
3	0.126	0.128
4	0.115	0.117
5	0.132	0.135

Results from the 100 km baseline are shown in Table 5.4. The addition of C/A code observations on the 100 km baseline caused a slight decrease in the uncertainty of the parameter estimates, compared with the solution using only phase observations. For the 10 km baseline, the parameter estimate uncertainties did not decrease. The large uncertainties of the bias parameters prevented any biases from being fixed to an integer value.

Table 5.4 100 km baseline uncertainties in parameter estimates

Parameters	L1 + L2 Uncertainty $(3*\sigma_{uncertainty}*\chi_v^2)$	L1 + L2 + C/A Uncertainty $(3*\sigma_{uncertainty}*\chi_v^2)$
Latitude (rad)	0.13×10^{-6} (0.015m)	0.13×10^{-6} (0.015m)
Longitude (rad)	0.35×10^{-6} (0.035m)	0.35×10^{-6} (0.034m)
Radius (km)	0.32×10^{-4} (0.032m)	0.31×10^{-4} (0.031m)
L1 Bias (L1 cycles):		
1	1.75	1.72
2	1.81	1.78
3	1.85	1.82
4	1.75	1.72
5	1.94	1.90
L2-L1 Bias (L2-L1 cycles):		
1	0.502	0.492
2	0.519	0.508
3	0.530	0.520
4	0.501	0.491
5	0.552	0.541

Results from the 330 km baseline were qualitatively similar to the 10 km baseline results, but the magnitude of the uncertainties themselves were much larger. The results are not presented here. The coordinate uncertainties were several centimeters, and the bias parameter uncertainties were approximately 4 cycles for the L2-L1 biases and around 14 cycles for the L1 biases. No biases were able to be fixed for this baseline.

To account for the lack of improvement from the addition of C/A code observables, further tests were performed to examine the accuracy of the C/A code simulation. The standard deviation of random noise for the simulated double difference C/A code observations was reduced from 2 m to 20 cm, and the observations were processed for the 10 km baseline.

The resulting solution showed an increase in the uncertainties, instead of a decrease. The value of χ_v^2 increased from approximately 1, with 2 m rms noise, to 3.27. This increase in χ_v^2 indicates that the assumed 20 cm assumed *a priori* standard deviation for the C/A code was less than the actual standard deviation of the simulated observations. By reducing the assumed *a priori* standard deviation on the C/A code, the weight of these observations were greater, allowing the unmodeled sources to corrupt the baseline measurement. Using C/A code observations with 2 m rms noise, and setting the assumed a *priori* standard deviation accordingly, significantly reduces the weight of the pseudorange observations relative to the phase observations. The lower weight reduces the effect of the unmodeled errors in the C/A code data on the baseline measurement.

The role of the ionospheric contribution was further studied, to account for results presented above. Although the effect of the ionosphere on pseudorange and phase observables is equal and opposite, the ability to retrieve information on the ionosphere from each observable differs. Due to integer ambiguity present in the double difference phase observable, it is difficult to get a accurate estimate for the ionospheric parameter, without fixing the biases. Pseudorange observables do not contain an ambiguity parameter, making it possible to get an accurate estimate of ionospheric parameter (k). The C/A code observations are only available at a single frequency, reducing its potential for estimating the ionospheric parameter. Pseudorange observations at both the L1 and L2 frequencies would allow a more accurate estimation of the ionospheric contribution.

Further test cases were run to determine the viability using the ionospheric information on the C/A code to constrain the estimation of the ionosphere. This was tested by loosening the constraint on the ionosphere (i.e. increasing σ_{ion}) to 1000 ppm, on the 10 km baseline. Phase observations were processed with pseudorange observations, having 2 m and 20 cm of rms random noise. The two test cases are listed in Table 5.5.

Table 5.5 Assumed a *priori* standard deviation for two test cases

	Case 1	Case 2
Phase observations	2.9 mm	2.9 mm
C/A code observations	2000 mm	200 mm
Ionospheric contribution	1000 ppm	1000 ppm

Using C/A code observations with 2 m rms random noise, parameter estimates were similar to those obtained using only L1 and L2 phase observations with a tighter ionospheric constraint (8 ppm). This can be attributed to the small weight given the C/A code relative to phase observations. The value of χ_v^2 was 1.04. The uncertainty of the integer bias parameters increased by a factor of 100, reflecting the large a *priori* ionospheric contribution uncertainty. The large a *priori* uncertainty implies that the L1 and L2 phase observables are being combined into an LC observable, resulting in bias parameters which are highly correlated. For the second case, C/A code observations with 20 cm of measurement error were processed with phase observations. It was hoped that in this case, by increasing the weight of the pseudorange observable, the ionospheric error estimate would improve. Instead, results similar to previous case were obtained, except that the uncertainties in the position coordinates were larger by 50 % and χ_v^2 increased to 3.25. These results indicate that the C/A code observable does not improve estimation of the ionospheric error.

6.0 Conclusions

This study indicates that addition of the C/A code does not improve the estimation of baseline parameters. This statement must be taken cautiously, since there are several sources of error in this study. Two primary sources of weakness are the lack of an *a priori* model for the ionosphere, and the simulation of C/A code observations. The lack of an *a priori*, parameterized, ionosphere model prevented the ionospheric contribution from being more thoroughly removed from the observations. The use of an imperfect ionosphere model for the mean value of the ionosphere, introduced errors in the simulated C/A code, which were inconsistent with the phase observations. It has proved to be difficult to make the simulated C/A code observations as realistic and consistent with the phase observations.

It appears that pseudorange information is redundant for short baselines, since the integer ambiguity parameters can determined for such baselines. The pseudorange information is more valuable on the longer baselines. where it is difficult to fix the integer ambiguity parameters.

Acknowledgements

The author completed this work as a graduate research assistant in the Space Geodesy Group of the Center of Space Research. The work was supported by Air Force Contract F19628-86-K-0009 with the Air Force Geophysics Laboratory. The GPS data was provided by Aero Service Division, Western Geophysical Company of America.

I would like to thank several people for their contribution throughout this study:

Appendix A

The elements of the weight matrix, for L1 and L2 phase only algorithm, are given below.

$$[W] = \begin{bmatrix} w_{11} & w_{12} \\ w_{21} & w_{22} \end{bmatrix} \tag{A.1}$$

$$w_1 = \frac{1}{\sigma_{L1}^2} \tag{A.2}$$

$$w_2 = \frac{1}{\sigma_{L2}^2} \tag{A.3}$$

$$w_3 = \frac{1}{\sigma_{C/A}^2} \tag{A.4}$$

$$w_4 = \frac{1}{\sigma_{ion}^2} \tag{A.5}$$

$$w_{11} = \frac{w_2(w_1 + w_4)g^4 + w_1(w_4 - 2w_2)g^2 + w_1 w_2}{(w_1 + w_4)g^2 + w_2} \tag{A.6}$$

$$w_{12} = \frac{w_4(w_1 + w_2)g^2}{(w_1 + w_4)g^2 + w_2} \tag{A.7}$$

$$w_{12} = w_{21} \tag{A.8}$$

$$w_{22} = \frac{w_4 (w_1 g^2 + w_2)}{(w_1 + w_4) g^2 + w_2} \tag{A.9}$$

The elements of the transformation matrix, for L1 and L2 phase only algorithm, are given below.

$$[T] = \begin{bmatrix} t_{11} & t_{12} \\ t_{21} & t_{22} \end{bmatrix} \tag{A.10}$$

$$t_{11} = \frac{1}{1 - g^2} \tag{A.11}$$

$$t_{12} = - \frac{g}{1 - g^2} \tag{A.12}$$

$$t_{21} = - \frac{g^2}{1 - g^2} \tag{A.13}$$

$$t_{22} = \frac{g}{1 - g^2} \tag{A.14}$$

Appendix B

The elements of the weight matrix, for L1 phase, L2 phase, and C/A code algorithm, are given below.

$$[W] = \begin{bmatrix} w_{11} & w_{12} \\ w_{21} & w_{22} \end{bmatrix} \qquad (B.1)$$

The the weight terms (w_1, w_2, w_3, and w_4) are defined in Appendix A, Equations A.2 through A.5.

$$w_{11} = \frac{w_2(w_1+w_3+w_4)g^4 + \left[(w_1+w_3)(2w_2+w_4)+4w_1w_3\right]g^2 + w_2(w_1+w_3)}{(w_1+w_3+w_4)g^2 + w_2} \qquad (B.2)$$

$$w_{12} = \frac{w_4(w_1+w_2-w_3)g^2}{(w_1+w_3+w_4)g^2 + w_2} \qquad (B.3)$$

$$w_{12} = w_{21} \qquad (B.4)$$

$$w_{22} = \frac{w_4(w_1+w_3)g^2 + w_2w_4}{(w_1+w_3+w_4)g^2 + w_2} \qquad (B.5)$$

The elements of the transformation matrix, for L1 and L2 phase only algorithm, are given below.

$$[T] = \begin{bmatrix} t_{11} & t_{12} & t_{32} \\ t_{21} & t_{22} & t_{32} \end{bmatrix} \qquad (B.6)$$

$$t_{11} = \frac{w_1(2w_3-w_2)g^2 + w_1w_2}{w_2(w_1+w_3)g^4 + 2\left[w_2(w_3-w_1)+2w_1w_3\right]g^2 + w_2(w_1+w_3)} \qquad (B.7)$$

46

$$t_{12} = \frac{w_2(w_1 + w_3)g^3 + w_2(w_1 - w_3)g}{w_2(w_1 + w_3)g^4 + 2\left[w_2(w_3 - w_1) + 2w_1 w_3\right]g^2 + w_2(w_1 + w_3)}$$

(B.8)

$$t_{13} = \frac{w_3(2w_1 + w_2)g^2 + w_2 w_3}{w_2(w_1 + w_3)g^4 + 2\left[w_2(w_3 - w_1) + 2w_1 w_3\right]g^2 + w_2(w_1 + w_3)}$$

(B.9)

$$t_{21} = \frac{w_1 w_2 g^4 + 2(w_3 - w_2)g^2}{w_2(w_1 + w_3)g^4 + 2\left[w_2(w_3 - w_1) + 2w_1 w_3\right]g^2 + w_2(w_1 + w_3)}$$

(B.10)

$$t_{22} = \frac{w_2(2w_3 - w_1)g^3 + w_2(w_1 + w_3)g}{w_2(w_1 + w_3)g^4 + 2\left[w_2(w_3 - w_1) + 2w_1 w_3\right]g^2 + w_2(w_1 + w_3)}$$

(B.11)

$$t_{23} = -\frac{w_2 w_3 g^4 + (2w_1 + w_2)g^2}{w_2(w_1 + w_3)g^4 + 2\left[w_2(w_3 - w_1) + 2w_1 w_3\right]g^2 + w_2(w_1 + w_3)}$$

(B.12)

The extra term (c) in Equation 4.47 is:

$$c = \frac{w_1 w_2 w_3 \left[\phi_{L1}(1 + g^2) - 2\phi_{L2}g - \phi_{C/A}(1 - g^2)\right]}{w_2(w_1 + w_3)g^4 + 2\left[w_2(w_3 - w_1) + 2w_1 w_3\right]g^2 + w_2(w_1 + w_3)}$$

(B.13)

Note that all the elements of the transformation matrix and the extra term (c) have the same

denominator. The extra term is zero if any of the weights are equal to zero.

References

Abbot, R.I., C.C. Counselman III, and S.A. Gourevitch, "GPS Orbit Determination: Bootstrapping to Resolve Carrier Phase Ambiguity', Presented at the *Fifth International Geodetic Symposium on Satellite Positioning*, New Mexico State University, Las Cruses, March 13-17, 1989.

Beutler, G., et.al., "Using the Global Positioning System (GPS) for High Precision Geodetic Surveys: Highlights and Problem Areas", *IEEE PLANS '86: Positions Location and Navigation Symposium*, pp. 243-250, November 19' 6.

Bevington, P.R., *Data Reduction and Error Analysis for the Physical Sciences*, McGraw-Hill Book Co.,New York, NY, 1969.

Colombo, O.L., "Ephemeris Errors of GPS Satellites", *Bulletin Geodesique*, vol. 60, pp. 64-84, 1986.

Counselman III, C. C., et. al., "Accuracy of Baseline Determinations by MITES Assessed by Comparison with Tape, Theodolite, and Geodimeter Measurements", *EOS, the Transactions of the American Geophysical Union*, vol. 62, p. 260, April 28, 1981.

Counselman III, C.C., R.I. Abbot, "An Improved Strategy for Determining Earth Satellite Orbits by Radio", (to be published in *Journal of Geophysical Research*).

Counselman III, C. C., S.A. Gourevitch, "Miniature Interferometer Terminals for Earth Surveying: Ambiguity and Multipath with Global Positioning System", *IEEE Transactions on Geoscience and Remote Sensing*, vol. GE-19, no. 4, pp. 244-252, October 1981.

Counselman III, C. C., J.W. Ladd, "A Dual-Band Interferometric GPS Marine Navigation System", *Proc. International Symposium on Marine Positioning: Positioning the Future*, pp. 197-214, Reston, VA, October 1986.

Hatch, R., "The synergism of GPS code and carrier measurements", *Proc. Third International Geodetic Symposium on Satellite Doppler Positioning*, vol. 2, pp. 1213-1231, New Mexico State University, Las Cruses, 1982.

King, R.W., E.G. Masters, C. Rizos, A. Stolz, and J. Collins, *Surveying with GPS* , Monograph No. 9, School of Surveying, University of New South Wales, Kensington, N.S.W., Australia, November 1985.

Ladd, J.W., R.G. Welshe, "Mini-Mac™ - A New Generation Dual-Band Surveyor", *Prcc. Fourth International Geodetic Symposium on Satellite Positioning*, vol. 2, pp. 475-487, University of Texas, Austin, 1986.

Lichten,S.M., and J.S. Border, "Strategies for High-Precision Global Positioning System Orbit Determination", *Journal of Geophysical Research*, vol. 92, pp. 12751-12762, 1987.

Rawer, K., D. Bilitza, "Study of Ionospheric and Tropospheric Models", *NASA Report N86-26750*, 1985.

Remondi, B.W., "Using the Global Positioning System (GPS) phase observable for relative geodesy: modeling, processing, and results", *Ph.D. Dissertation*, Center for Space Research, The University of Texas at Austin, 1984.

Solloway, C.B., *Elements of the Theory of Orbit Determination*, JPL Engineering Planning Document, No. 225, December 1964.

Spilker, J. J., "GPS signal structure and performance characteristics", *Global Positioning System*, The Institute of Navigation, vol. 1, pp. 29-54, 1980.

Strang, G., *Linear Algebra and its Applications*, Academic Press, Inc., New York, NY, 1980.

Wubbena, G., A. Schuchardt, and G. Seeber, "Multistation positioning results with TI4100 GPS receivers in geodetic control networks", *Proc. Fourth International Geodetic Symposium on Satellite Positioning*, vol. 2, pp. 963-978, University of Texas, Austin, 1986.